9
Quantum Information Processing with Atom Chips

Philipp Treutlein, Antonio Negretti, and Tommaso Calarco

9.1
Introduction

Since the 1990s, when groundbreaking algorithms based on the laws of quantum mechanics for solving classically intractable computational problems were found, quantum information science has rapidly grown with the promise of building a quantum computer. Similar to present 'classical' computers, quantum hardware consists of memory and a processor. The former stores the information, the latter, with a set of gates, processes the information.

The concept of gate is fundamental in quantum computation [1]. Thus, let us first consider its classical analogue. A gate in a classical computer, which implements a Boolean function, is a device that accomplishes a well-defined operation on one or more bits. For instance, CMOS transistors realize the logical NOT operation. Instead, a quantum gate performs a unitary operation on the linear space of quantum bits (*qubits*). Thus, a quantum gate is the time evolution operator generated by a given Hamiltonian; control by external fields, according to the Hamiltonian structure, allows one to perform desired transformations on the qubit wave function. In the 1990s it was shown that a general N-qubit gate can be decomposed into $O(N^2)$ one- and two-qubit gates. Because of this crucial theoretical result, most of the schemes for quantum gates concern the implementation of one- and two-qubit operations, which will be the main topic of this chapter.

Atom chips combine many important features of a scalable architecture for quantum information processing (QIP): (1) the exquisite coherence properties of neutral atoms; (2) accurate control of the coherent evolution of the atoms in tailored micropotentials; (3) scalability of the technology through microfabrication, which allows the integration of many qubits in parallel on the same device while maintaining individual addressability; (4) interfaces to photons as flying qubits provided by on-chip optical cavities; and (5) the exciting perspective of interfacing quantum optical qubits with solid-state systems for QIP located on the chip surface. In this respect, the unique features of atom chips such as trap miniaturization and integration are powerful concepts from which many different systems can benefit, as

Atom Chips. Edited by Jakob Reichel and Vladan Vuletić

ISBN: 978-3-527-40755-2

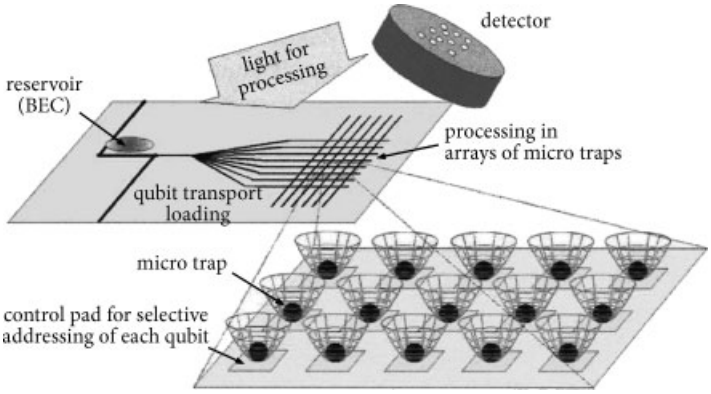

Figure 9.1 Schematic illustration of an atom chip quantum processor, adapted from [2].

the current efforts to miniaturize ion traps, initiated by the success of neutral atom chip traps, show.

Figure 9.1 illustrates the general idea of an atom-chip-based quantum information processor. It includes a reservoir of cold atoms, preferably in their motional ground state, and in a well-defined internal state. An ideal starting point for this is a BEC (Bose–Einstein condensate) in a chip trap. From there the atoms are transported using guides or moving potentials to a large array of processing sites. Either single atoms, or small ensembles of atoms, are then loaded into the qubit traps. Each qubit site can be addressed individually. Micro-fabricated wires and electrodes located close to the individual sites can be used for site-selective manipulations such as single-qubit gates. For two-qubit gates, interactions between adjacent sites are induced. For readout, micro-optics can be used to focus lasers onto each site separately, or the whole processor can be illuminated and single qubits are addressed by shifting them in and out of resonance using local electric or magnetic fields.

9.2 Ingredients for QIP with Atom Chips

A fully developed architecture for quantum information processing with atom chips comprises the following ingredients [2–4]:

1. **Qubit states with long coherence lifetime.** A qubit state pair has to be identified which can be manipulated with electromagnetic fields on the chip, but still allows for long coherence lifetimes in a realistic experimental situation. In particular, attention has to be paid to decoherence and loss mechanisms induced by the chip surface, which is typically at a distance of only a few micrometers from the atoms.

2. **Qubit rotations (single-qubit gates).** High-fidelity single-qubit rotations have to be implemented. This corresponds to high-contrast Rabi oscillations between the qubit states, with a period much shorter than the coherence lifetime.
3. **Single-qubit readout.** Individual qubits have to be read out with high efficiency. Since most scenarios for QIP with atom chips implement the qubit in single atoms, this requirement amounts to single-atom detection – ideally with a detector which is integrated on the chip.
4. **Single-qubit preparation.** A method has to be developed to deterministically prepare single qubits on the chip. In most proposals, this amounts to deterministic single-atom preparation. An exception are ensemble-based approaches to QIP. Furthermore, many proposals require the atoms to be prepared in the motional ground state of the trap, with very low occupation probability of excited states.
5. **Conditional quantum dynamics (two-qubit gates).** A universal two-qubit quantum gate is needed, which allows for high-fidelity gate operations under realistic conditions. A gate infidelity (error rate) below a certain threshold is required in order to allow for a fault-tolerant implementation of quantum computing. Depending on error models and recovery schemes, estimates of such a threshold vary from a few 10^{-3} for active error correcting codes [5] up to well above 10 % for error detection schemes [6].
6. **Interfaces to other systems.** Interfaces allow one to transfer quantum information from the atoms to other physical systems. One example is an interface between atoms for processing and storage and photons (optical or microwave) for transmission of information. Furthermore, quantum interfaces are the key ingredient of hybrid approaches to QIP, where the gate operations themselves rely on the coupling of atoms to ions, molecules, or solid-state quantum systems such as Cooper pair boxes and superconducting microwave cavities.

In the following sections, we discuss each point of the above list. We highlight the main challenges, review theoretical proposals which show how these ingredients can be implemented on atom chips, and report on the status of experimental realizations.

9.3
Qubit States with Long Coherence Lifetime

Two potentially conflicting requirements have to be met by the qubit states $\{|0\rangle, |1\rangle\}$ chosen for QIP on atom chips. On the one hand, both states have to couple to the electromagnetic fields which are used for trapping and manipulating the atoms. On the other hand, high-fidelity gate operations require a long coherence lifetime of superposition states $\alpha|0\rangle + \beta|1\rangle$, ($|\alpha|^2 + |\beta|^2 = 1$), and thus the qubit has to be sufficiently robust against fluctuations of electromagnetic fields in realistic experimental situations. A peculiarity of chip-based traps is the presence of atom–surface interactions, which lead to additional loss and decoherence mechanisms

which are not present in macroscopic traps (see Chapters 4 and 5). It is therefore important to investigate the coherence properties of the proposed qubit candidates close to the chip surface. In the following we discuss the different types of qubits which have been studied.

Hyperfine Qubits

An obvious qubit candidate are the long-lived ground-state hyperfine levels of the atoms. In most experiments, at least a part of the trapping potential is provided by static magnetic fields generated by wires or permanent-magnet structures on the atom chip. It is, therefore, desirable that both $|0\rangle$ and $|1\rangle$ are magnetically trappable. Long coherence lifetimes can be expected if states with equal magnetic moments are chosen, so that both states experience nearly identical trapping potentials in static magnetic traps, and the energy difference $h\nu_{10} = E_{|1\rangle} - E_{|0\rangle}$ between $|0\rangle$ and $|1\rangle$ is robust against magnetic field fluctuations. These requirements are satisfied by the $|F = 1, m_F = -1\rangle \equiv |0\rangle$ and $|F = 2, m_F = +1\rangle \equiv |1\rangle$ hyperfine levels of the $5S_{1/2}$ ground state of ^{87}Rb.

In [7], the coherence properties of this qubit were studied experimentally on an atom chip. Figure 9.2 shows measurements of the coherence lifetime close to the chip surface. The atoms were held in a magnetic trap, with a magnetic field of $B_0 \sim 3.23$ G in the trap center. At this field, both states experience the same first-order Zeeman shift and the remaining magnetic field dependence of the transition frequency ν_{10} is minimized. The coherence lifetime was measured at different atom–surface distances d using Ramsey spectroscopy. Coherence lifetimes exceeding 1 s were observed, comparable to those obtained in macroscopic traps. Within the experimental error, the Ramsey contrast does not show a dependence on atom–surface distance for $d = 5$–130 μm. These experiments confirm that this hyperfine qubit is very well suited for atom chip-based QIP. It is, therefore, considered in several schemes for atom chip quantum gates (see Section 9.7). Large arrays

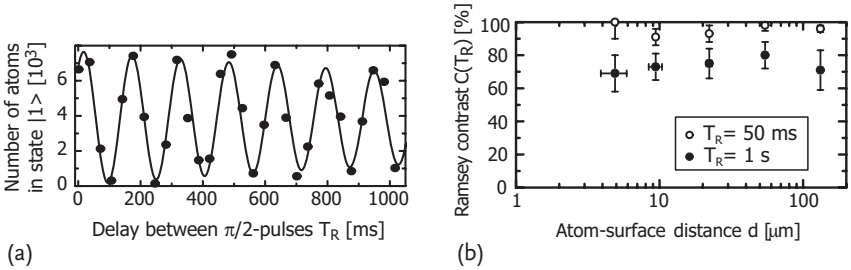

Figure 9.2 Coherence lifetime measurements of the hyperfine qubit $|F = 1, m_F = -1\rangle \equiv |0\rangle$ and $|F = 2, m_F = +1\rangle \equiv |1\rangle$ (adapted from [7]). (a) Ramsey spectroscopy of the $|0\rangle \leftrightarrow |1\rangle$ transition with atoms held at a distance $d = 9$ μm from the atom chip surface. An exponentially damped sine fit to the Ramsey fringes yields a $1/e$ coherence lifetime of $\tau_c = 2.8 \pm 1.6$ s. Each data point corresponds to a single shot of the experiment. (b) Contrast $C(T_R)$ of the Ramsey fringes as a function of d for two values of the time delay T_R between the $\pi/2$-pulses.

of qubits could be prepared in chip-based magnetic lattice potentials which are demonstrated in [8, 9].

Magnetic-field-insensitive hyperfine qubits were also experimentally studied in optical microtraps, created by an array of microlenses [10]. Using spin-echo techniques, coherence times of 68 ms were obtained, limited by spontaneous scattering of photons. Simultaneous Ramsey measurements in up to 16 microtraps were performed, demonstrating the scalability of this approach.

Vibrational Qubits

Qubits can also be encoded in the vibrational states of atoms in tight traps. This has been proposed both for optical [11, 12] and magnetic [13, 14] microtraps. The computational basis states can be two vibrational levels in a single trap, for example the ground and first excited vibrational level [11]. Alternatively, they can be defined by the presence of an atom in either the left or the right well of a double-well potential [12]. Initialization of the atoms in the lowest vibrational state of the trap with high fidelity is crucial in both of these schemes.

Vibrational states are usually more delicate to handle and to detect than hyperfine states. An advantage, on the other hand, is that an internal-state independent interaction is sufficient for two-qubit gates and collisional loss can be reduced as the two interacting qubits are in the same internal state. The proposals of [13, 14], therefore, consider a combination of hyperfine states for qubit storage and vibrational states for processing. Measurements of vibrational coherence near surfaces still have to be performed. The expected fundamental limits due to surface-induced decoherence, however, are comparable to those for hyperfine states (see Chapters 4 and 5).

Rydberg State Qubits

Rydberg states are attractive for QIP because of their strong electric dipole moment [15, 16]. The resulting dipole–dipole interaction between Rydberg atoms can be exploited for fast two-qubit quantum gates. Moreover, Rydberg qubits can be combined with long-lived ground state hyperfine qubits for information storage. For the $n \sim 50$ Rydberg states of Rb, typical lifetimes are $\sim 100\,\mu$s for low angular momentum states up to ~ 30 ms for circular states. In [16] it is proposed to enhance the lifetime of circular Rydberg states into the range of seconds by using a micro-structured trap on a superconducting atom chip that simultaneously acts as a cavity with a microwave cut-off frequency high enough to inhibit spontaneous emission. Furthermore, it is shown that with the help of microwave state dressing, coherence lifetimes of similar magnitude could be achieved.

Ensemble-Based Qubits

A single qubit can be encoded in collective states of an ensemble of particles [17, 18]. State $|0\rangle$ corresponds to all particles in the ground state, while in state $|1\rangle$, a single excitation is shared collectively by the whole ensemble. To isolate this two-level system, a blockade mechanism is required that prevents the creation of two or more excitations. The necessary nonlinearity can be provided by the dipole–dipole

interaction of Rydberg atoms [17–19], or by coupling the ensemble via a cavity to a single saturable two-level system such as a Cooper pair box [20, 21]. Ensemble qubits have the advantage that single-atom preparation is not required. Moreover, the Rabi frequency between the collective qubit states is enhanced by $\sqrt{N}$, where N is the number of atoms in the ensemble. The decay rates are the same as for a single particle if the decay is dominated by non-collective processes such as atom loss. Ensemble qubits in chip traps have been considered for ground-state atoms [21], Rydberg atoms [19], and polar molecules [20, 22].

Hybrid Systems Involving Solid-State Qubits

A particularly attractive feature of chip traps is the possibility to combine atomic or molecular qubits with solid-state qubits on the chip surface [20–24]. Such hybrid systems would combine fast processing in the solid state with long coherence times for information storage in the atomic system. An impressive degree of coherent control has been demonstrated for example for qubits based on superconducting circuits [25, 26]. Coherent dynamics as well as decoherence in these systems typically occur on a time scale of nanoseconds to microseconds, several orders of magnitude faster than in atomic gases. A very promising approach to couple atomic and superconducting qubits is the use of superconducting microwave resonators [20–22, 24]. To combine the necessary cryogenic technology with atom chips represents an experimental challenge which is currently pursued in several experiments.

9.4 Qubit Rotations (Single-Qubit Gates)

Single-qubit gates are unitary transformations in the Hilbert space of a single qubit. In the language of atomic physics, this corresponds to rotations on the Bloch sphere of the two-level system encoding the qubit. The necessary degree of control can be experimentally demonstrated by driving high-contrast Rabi oscillations between the qubit states. Atom-chip-based experiments have demonstrated such control with hyperfine qubit states. Coherent control of motional states has been demonstrated in the context of atom interferometry.

Hyperfine Qubits

Hyperfine qubit states can be coupled with oscillating microwave and/or radio-frequency (rf) magnetic fields. High-fidelity Rabi oscillations on the qubit transition $|F = 1, m_F = -1\rangle \leftrightarrow |F = 2, m_F = +1\rangle$ of ^{87}Rb discussed in Section 9.3 have already been demonstrated experimentally on an atom chip, see Figure 9.3 and [7, 27]. In this case, a two-photon transition with a microwave and an RF photon is involved. A two-photon Rabi frequency of a few kHz is easily achieved, so that single-qubit gates can be performed on a time scale of hundreds of microseconds, three to four orders of magnitude faster than the relevant coherence lifetimes. Al-

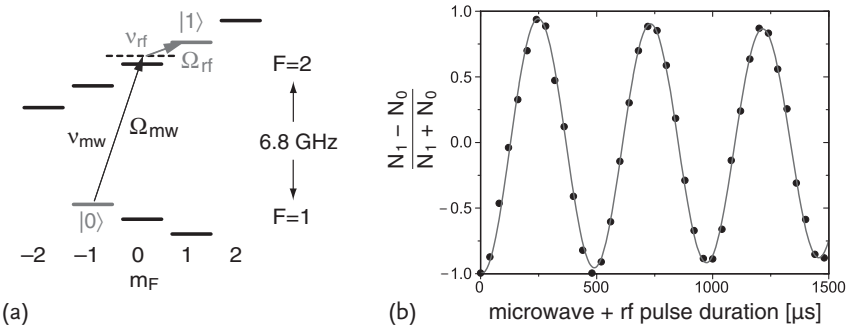

Figure 9.3 Qubit state rotations on the hyperfine transition $|F = 1, m_F = -1\rangle \equiv |0\rangle$ and $|F = 2, m_F = +1\rangle \equiv |1\rangle$ (adapted from [4]). (a) Ground-state hyperfine structure of ^{87}Rb in a weak magnetic field. The first-order Zeeman shift of the states $|0\rangle$ and $|1\rangle$ is approximately identical. The two-photon transition $|0\rangle \leftrightarrow |1\rangle$ is driven by a microwave ν_{mw} and a radio-frequency ν_{rf}. Ω_{mw} and Ω_{rf} are the single-photon Rabi frequencies of the microwave and RF transition, respectively. (b) Rabi oscillations on the two-photon transition recorded as a function of the microwave and RF pulse length. The two-photon Rabi frequency is $\Omega_{2ph}/2\pi = 2.1$ kHz, and the fidelity of a π-pulse is 96 %.

ternatively, hyperfine states can be coupled through a two-photon Raman transition driven by two laser beams [10, 28].

A nice feature of atom chips is that the qubit driving fields can be generated by chip-based waveguides (for microwaves) or just simple wires (for RF). This results in a stable, well-controlled coupling with tailored polarization. All elements for qubit manipulation can thus be integrated on chip. Moreover, chip-based driving fields can have strong near-field gradients. This is advantageous as it allows individual addressing of spatially separated qubits. On the other hand, care has to be taken to avoid dephasing due to strong gradients across a single qubit.

Vibrational Qubits

If the qubit is encoded in the ground and first excited vibrational levels of a single trap [11, 13, 14], qubit rotations can be induced by driving a two-photon Raman transition between the states with two lasers. Such transitions between vibrational levels are routinely employed in ion trap QIP [28] and have been demonstrated in optical dipole traps [29]. Similar experiments with neutral atoms in chip traps still have to be performed. As the vibrational levels have to be spectrally resolved, tight traps with large vibrational frequencies are required. On atom chips, sufficiently high vibrational frequencies of up to ~ 1 MHz are accessible.

If the qubit basis states are the left and right states of a double well [12], single-qubit gates can be performed by adiabatically lowering the barrier between the two wells and allowing tunneling to take place. This has strong connections to atom interferometry. Chip-based atom interferometers demonstrating versatile coherent control of the motional state of BECs have been realized, see for example [27, 30, 31] and Chapter 7.

Other Qubit Implementations

Several new atom chip experiments with relevance for QIP are currently being set up, involving among other things Rydberg atoms or superconducting structures on the chip (see Chapter 10). We expect chip-based experiments on coherent control in these systems in the near future.

9.5 Single-Qubit Readout (Single-Atom Detection)

Most schemes for QIP on atom chips consider individual atoms as the carriers of quantum information. While preparation, manipulation, and detection of single particles is a standard task in ion trap experiments, it is significantly harder to achieve with neutral atoms. This is because there is no equivalent to the strong Coulomb interaction that allows one to separate individual trapped ions, and that provides a tight, internal-state independent trapping potential in which the ions can be held during detection. The atom chip experiments on qubit state coherence and qubit rotations described in Sections 9.3 and 9.4, for example, were performed with atomic ensembles. While they indeed demonstrate the usefulness of the investigated states for QIP, eventually similar experiments will have to be performed with single atoms. An important achievement is therefore the integration of single-atom detectors with atom chip technology. In the following, we briefly highlight chip-based single-atom detectors which have been realized.

One approach to single-atom detection is photoionization and subsequent ion detection. This has been demonstrated on an atom chip in [32]. For atoms in Rydberg states, state-dependent electric field ionization is used as a standard single-atom detection method [16]. Detectors based on ionization are destructive, that is the atom is lost after detection. Fluorescence detection, which is also employed in ion trap experiments, can in principle provide non-destructive single-atom detection if the atom is held in a tight, state-independent trap such as an optical dipole trap. A simple and compact system for on-chip fluorescence detection are the fiber-based detectors demonstrated in [33].

High-finesse optical cavities are a particularly powerful system for single-atom detection. Non-destructive detection with negligible heating of atomic motion is possible. Moreover, optical cavities form the basis of certain quantum gate schemes, see Section 9.7.4, and of interfaces between storage qubits (atoms) and flying qubits (photons), see Section 9.8.2. An experiment demonstrating single-atom detectivity with a macroscopic cavity surrounding an atom chip is reported in [34]. Moreover, miniaturized optical cavities were developed which are directly integrated on the chip [35–38]. The single-atom strong coupling regime of cavity quantum electrodynamics was reached with such a cavity on an atom chip [37].

9.6
Single-Qubit Preparation (Single-Atom Preparation)

The availability of single-atom detectors on atom chips enables experiments on deterministic single-atom preparation. In many proposals for QIP, single atoms have to be prepared in the vibrational ground state of the trapping potential with very high probability – either because the qubit itself is encoded in vibrational states, or because atomic motion plays a crucial role in two-qubit gates, for example in the form of collisions between atoms.

A BEC can be seen as a large reservoir of atoms in the motional ground state. Proposals for the deterministic extraction of single atoms from a BEC have been made [39, 40]. They consider a tight microtrap into which condensate atoms can be transferred. Precise control of the atom number in the tight trap is provided by a collisional blockade mechanism. This is related to the Mott insulator transition, which could be used to prepare a large array of single atoms in an on-chip lattice. An alternative is heralded single-atom preparation, where atoms are probabilistically coupled from a BEC reservoir to an initially unoccupied internal state, which is continuously monitored with a non-destructive single-atom detector such as an optical cavity. Once an atom is detected, the coupling is turned off.

Single neutral atoms can already be prepared by loading an optical dipole trap from a magneto-optical trap, exploiting again collisional blockade [41]. This approach could be used for optical microtraps. Initially, the atoms are thermally distributed over many vibrational states. Raman sideband cooling could be used for ground-state cooling.

9.7
Conditional Dynamics (Two-Qubit Gates)

Two-qubit gates are the heart of a quantum processor, as they are required for the generation of entanglement between the qubits. In this section we present schemes for two-qubit gates that can be implemented with neutral atoms on an atom chip.

Let us consider the dynamics of an arbitrary number of atoms (no matter if charged or not) in a time- and state-dependent three-dimensional trapping potential $V_k(\boldsymbol{r}, t)$, $\boldsymbol{r} = (x, y, z)$ governed by the Hamiltonian operator [42, 43]

$$\hat{H}(t) = \sum_{k=0}^{1} \int \mathrm{d}\boldsymbol{r}\, \hat{\Psi}_k^\dagger(\boldsymbol{r}) \left[-\frac{\hbar^2}{2m} \nabla^2 + V_k(\boldsymbol{r}, t) \right] \hat{\Psi}_k(\boldsymbol{r}) + \sum_{k,\ell=0}^{1} \frac{1}{2} \int \mathrm{d}\boldsymbol{r}\mathrm{d}\boldsymbol{r}'\, \hat{\Psi}_k^\dagger(\boldsymbol{r})\, \hat{\Psi}_\ell^\dagger(\boldsymbol{r}')\, U_{k\ell}(\boldsymbol{r}, \boldsymbol{r}')\, \hat{\Psi}_\ell(\boldsymbol{r}')\, \hat{\Psi}_k(\boldsymbol{r}) \,. \tag{9.1}$$

Here m is the atomic mass, $\hat{\Psi}_k^\dagger(\boldsymbol{r})$, $\hat{\Psi}_k(\boldsymbol{r})$ are atomic field creation and annihilation operators for the logic state $|k\rangle$, and $U_{k\ell}(\boldsymbol{r}, \boldsymbol{r}')$ is the two-atom interaction potential for the qubit states $|k\rangle$ and $|\ell\rangle$, with $k, \ell = 0, 1$. Our goal is the realization of a two-

qubit gate with two atoms, each of them carrying a qubit of information usually encoded in an extra degree of freedom (e.g., a pair of hyperfine states) other than their motional state. In this specific case, the full many-body problem described by the Hamiltonian (9.1) can be reduced to a Schrödinger equation for two trapped particles and this will be assumed in the following.

The quantum gate we aim to implement is a phase gate having the following truth table: $|\epsilon_1\rangle|\epsilon_2\rangle \rightarrow \mathrm{e}^{\mathrm{i}\phi\epsilon_1\epsilon_2}|\epsilon_1\rangle|\epsilon_2\rangle$, where $|\epsilon_1\rangle$, $|\epsilon_2\rangle$ are the logic qubit states with $\epsilon_{1,2} = 0, 1$. When the phase ϕ takes on the value of π, the combination of a phase gate with two Hadamard gates yields a controlled-NOT gate. In this respect it is an important quantum gate. Since it requires only to produce a phase shift for the state $|1\rangle|1\rangle$ such a gate has become of interest, because it requires a state-dependent interaction that is relatively straightforward to realize physically.

Let us explain the basic principle to obtain a conditional phase shift ϕ when two atoms are trapped in a microscopic potential. Initially, at $t = 0$, we assume that the two particles are in the respective ground states of the trapping potential and that their wave functions are well separated from each other so that their overlap is negligible. At times $0 < t < T_\mathrm{g}$ the potential wells are changed in such a way that the atomic wave functions are displaced differently depending on their logical state $|k\rangle$ and a state-dependent wave function overlap results. The particles interact for a time T_g, the gate operation time, and at $t = T_\mathrm{g}$ the initial situation is restored. With this approach we get state-dependent phase shifts of two kinds: a purely kinematic one, $\theta_k + \theta_\ell$, due to the single particle motion in the trapping potential; and an interaction phase, $\theta_{k\ell}$, due to the coherent interactions among the atoms. Thus, we can summarize the ideal phase gate with the mapping [43, 44]

$$|\epsilon_1\rangle|\epsilon_2\rangle|\psi_{\epsilon_1\epsilon_2}\rangle \rightarrow \mathrm{e}^{\mathrm{i}\phi\epsilon_1\epsilon_2}|\epsilon_1\rangle|\epsilon_2\rangle|\psi_{\epsilon_1\epsilon_2}\rangle, \tag{9.2}$$

where the motional state $|\psi_{\epsilon_1\epsilon_2}\rangle$ has to factor out at the beginning and at the end of the gate operation. In the ideal transformation (9.2) we grouped together the kinematic and global two-particle phases. Indeed, the application of single-qubit operations affords $\phi = \theta_{11} - \theta_{01} - \theta_{10} + \theta_{00}$ [45].

We conclude this section by introducing the concept of gate fidelity $F \in [0, 1]$, which will be a useful quantity later in the chapter to assess the gate performance. Basically, it is the projection of the physical state obtained by actually manipulating the system onto the logical state that the gate aims to attain, averaged over degrees of freedom (e.g., motion) that cannot be accurately controlled.

9.7.1
Internal-State Qubits and Collisional Interactions

In order to obtain conditional dynamics, as we discussed in the previous section, either the trapping potential or the interaction term should be state-dependent. In the case of ultra-cold neutral atoms, the interaction between atoms is mediated by two-body collisions, whose dominant contribution is s-wave scattering described

by

$$U_{k\ell}(\boldsymbol{r}, \boldsymbol{r}') = \frac{4\pi\hbar^2 a_{\mathrm{s}}^{k\ell}}{m}\delta^3\left(\boldsymbol{r} - \boldsymbol{r}'\right) \ , \tag{9.3}$$

where $a_{\mathrm{s}}^{k\ell}$ is the s-wave scattering length for the internal states $|k\rangle$ and $|\ell\rangle$. Because of the short range of the pseudopotential (9.3), the wave functions of the atoms have to overlap in order to interact, and for identical atoms in the same logical state, s-wave scattering is only possible for bosons, and therefore in the following we will consider bosonic atomic species. As the potential given in Eq. (9.3) assumes elastic collisions, the states $|0\rangle$ and $|1\rangle$ have to be chosen such that they remain the same after the collision.

One of the most effective theoretical models for an atom chip phase gate has been proposed in [42]. In this scheme the control of the interaction between the atoms is realized by changing the shape of a microscopic potential depending on the internal state of the atoms. Three conditions are assumed: (i) the shape of the potential is harmonic; (ii) the atoms are initially cooled to the vibrational ground state of two potential wells centered at $\boldsymbol{r} = \boldsymbol{r}_0$ and $\boldsymbol{r} = -\boldsymbol{r}_0$; (iii) the change in the form of the trapping potential is instantaneous. The principle of the gate is the following: at time $t = 0$ the barrier between the atoms, say in the x-direction, is suddenly removed (selectively) for atoms in the logical state $|1\rangle$, whereas for atoms in state $|0\rangle$ the potential is not changed. An atom in state $|1\rangle$ finds itself in a new harmonic potential centered at $\boldsymbol{r} = 0$ with a frequency ω, smaller than the one of the separated wells, ω_0. The atoms in state $|1\rangle$ are allowed to perform an integer number of oscillations and at $t = T_{\mathrm{g}}$ the initial wells are restored. In this process the particles acquire both a kinematic phase due to their oscillations in the traps and an interaction phase due to their collisions. In the tight transverse confinement regime, where the frequency ($\omega_\perp$) of the well in the y-z-directions is much larger than that (ω, ω_0) in the x-direction, the gate dynamics can be well approximated by a one-dimensional model with a contact potential $U_{k\ell}^{\mathrm{1D}}(x, x') = 2\hbar\omega_\perp a_{\mathrm{s}}^{k\ell}\delta(x - x')$. The kinematic phase $2n\pi\omega_\perp/\omega$ ($T_{\mathrm{g}} = 2\pi n/\omega$, $n \in \mathbb{N}$) due to the radial confinement is common to all states, while the one due to the oscillation in the axial direction is state-dependent. Because of the harmonicity of the trapping potentials, almost perfect revivals of the wave packet occur. By choosing $\omega = j\,\omega_0$, with $j \in \mathbb{N}$, and in the limit where the interaction does not induce any relevant alteration in the shape of the two-particle wave function, the gate operation time T_{g} can be fixed by looking at the revival where the total accumulated phase ϕ assumes a defined value, for example, π. Because of the form of $U_{k\ell}^{\mathrm{1D}}$ the frequency $\omega_\perp$ can be adjusted in order to fix the value of ϕ [42].

Atom chips can provide microscopic state-dependent potential landscapes in which atoms can be trapped and manipulated for the implementation of the above scheme. In [2] it was pointed out that a combination of static magnetic and static electric fields could be used for this purpose. However, several issues have to be addressed that could prevent a successful experimental realization of the scheme discussed above: (i) the trapping potentials are usually anharmonic; (ii) the fidelity is strongly reduced by wave packet distortion due to undesired collisions in some of

the qubit basis states [42]; (iii) transverse excitations of the atoms can arise during the collisions if the ratio $\omega_\perp/\omega$ is not properly chosen for the 1D condition. Those processes would significantly reduce the gate fidelity.

An analysis of the limitations due to anharmonicity of the potentials is carried out in [46]. In that analysis a cubic and a quartic term is added to the harmonic potential in order to include the next leading order terms in the Taylor series expansion of an arbitrary potential. While a cubic anharmonicity is well tolerated, the quartic correction poses severe restrictions to the correct performance of the gate that are not easy to satisfy on atom chips. Thus, for a correct performance, the atoms have to be forced to a given dynamics.

The variant of [47] to the original proposal [42] can be regarded as the first attempt towards a realistic implementation of the collisional phase gate on an atom chip. It employs the hyperfine qubit states $|0\rangle \equiv |F = 1, m_F = -1\rangle$ and $|1\rangle \equiv |F = 2, m_F = 1\rangle$ of ^{87}Rb whose favorable coherence properties were already discussed in Section 9.3. Moreover, its key ingredient, the coherent manipulation of these states with a state-dependent trapping potential, was realized in a recent experiment [27]. Let us analyze the features of this scheme (see Figure 9.4). The state-dependent potential is split into

$$V_k(\boldsymbol{r}, t) = u_c(\boldsymbol{r}) + \lambda(t) u_k(\boldsymbol{r}) \,, \tag{9.4}$$

where $u_c(\boldsymbol{r})$ is a common part and $u_k(\boldsymbol{r})$ a qubit-state-dependent part ($k = 0, 1$). The common part of the potential is a time-independent double-well potential along x that can be realized by a static magnetic potential, which is nearly identical for the chosen qubit states. As in [42], the dynamics can be reduced to 1D assuming a tight confinement in the transverse dimensions y, z. The state-dependent part can be realized by a microwave near-field potential (see below). It is modulated with a function $\lambda(t)$, with $0 \le \lambda(t) \le 1$. At times $t < 0$, when the gate is in its initial state, we have $\lambda(t) = 0$ and the atoms are subject to $u_c(\boldsymbol{r})$ only. Each atom is prepared

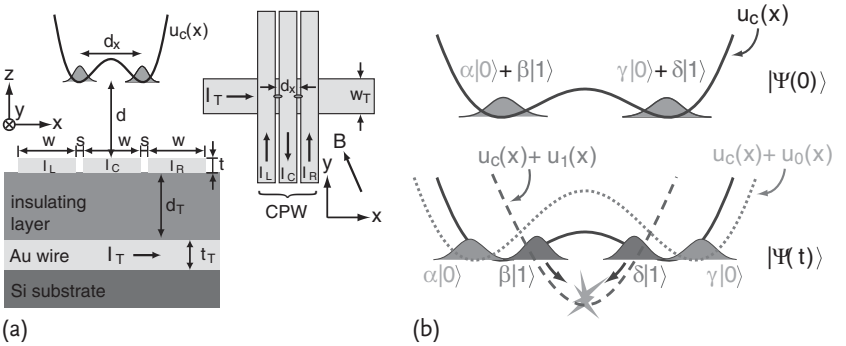

Figure 9.4 (a) Layout of the atom chip for the microwave collisional phase gate. (b) State-selective potential, atomic wave functions, and principle of the gate operation. Top: the state-independent potential $u_c(x)$ along the x direction. Bottom: the state-dependent potential $u_c(x) + u_k(x)$ (here $\lambda(t) = 1$). The atomic wave functions after half an oscillation period are shown.

in the motional ground of one of the wells of the double-well potential. During the time $0 \le t \le T_g$, $\lambda(t) \neq 0$ and the potential is state-dependent. The effect of $u_k(\boldsymbol{r})$ is twofold: $u_1(\boldsymbol{r})$ removes the barrier of the double well for state $|1\rangle$ and atoms in this state start to oscillate; the potential $u_0(\boldsymbol{r})$ shifts the minima of the double well for state $|0\rangle$ further apart in the x-direction (see Figure 9.4b), whereas in the original proposal those atoms do not experience any trap change. In this way, unwanted collisions (atoms in state $|01\rangle$), which are a major source of infidelity, are strongly reduced and the map (9.2) is implemented.

The state-dependent potential can be realized with microwave near-fields with a frequency near the hyperfine splitting of ^{87}Rb of 6.8 GHz. Unlike the optical potentials created by non-resonant laser beams, which can be tightly focussed due to their short wavelength, the centimeter wavelength λ_{mw} of microwave radiation poses severe limitations on far-field traps. On atom chips, however, the atoms are trapped at distances $d \ll \lambda_{mw}$ from the chip surface, and therefore they can be manipulated by microwave signals in on-chip transmission lines. In the near-field of the source currents and voltages, the microwave fields have the same position dependence as the static fields created by equivalent stationary sources. The maximum field gradients depend on the size of the transmission line conductors and on the distance d, not on λ_{mw}. Therefore, state-dependent microwave potentials varying on the micrometer scale can be realized. In a related way, radio-frequency fields can be used to generate near-field potentials (see Chapter 7).

When we consider the hyperfine levels $|F, m_F\rangle$ of the $5S_{1/2}$ ground state of a ^{87}Rb atom, the magnetic component of the microwave field $\boldsymbol{B}_{mw}(\boldsymbol{r})\cos(\omega t)$ couples the $|1, m_1\rangle$ to the $|2, m_2\rangle$ sublevels, with Rabi frequencies

$$\Omega_{1,m_1}^{2,m_2}(\boldsymbol{r}) = \frac{\langle 2, m_2|\hat{\boldsymbol{\mu}} \cdot \boldsymbol{B}_{mw}(\boldsymbol{r})|1, m_1\rangle}{\hbar} , \tag{9.5}$$

for the different transitions (in the rotating-wave approximation). In Eq. (9.5), $\hat{\boldsymbol{\mu}} = \mu_B g_J \hat{\boldsymbol{J}}$ is the operator of the electron magnetic moment ($g_J \simeq 2$). In a combined static magnetic and microwave trap, as considered here, both the static field $\boldsymbol{B}_s(\boldsymbol{r})$ and the microwave field $\boldsymbol{B}_{mw}(\boldsymbol{r})$ vary with position. This leads to a position-dependent microwave coupling with in general all polarization components present. The detuning of the microwave from the resonance of the transition $|1, m_1\rangle \to |2, m_2\rangle$ is:

$$\Delta_{1,m_1}^{2,m_2}(\boldsymbol{r}) = \Delta_0 - \frac{\mu_B}{2\hbar}(m_2 + m_1)|\boldsymbol{B}_s(\boldsymbol{r})| , \tag{9.6}$$

where $\Delta_0 = \omega - \omega_0$ is the detuning from the transition $|1, 0\rangle \to |2, 0\rangle$, and the different Zeeman shifts of the levels have been taken into account. The limit of large detuning $|\Delta_{1,m_1}^{2,m_2}|^2 \gg |\Omega_{1,m_1}^{2,m_2}|^2$ allows for long coherence lifetimes of the qubit states in the microwave potential. In this limit, the magnetic microwave potentials for the sublevels of $F = 1$ (left) and $F = 2$ (right) are given by

$$V_{mw}^{1,m_1}(\boldsymbol{r}) = \frac{\hbar}{4}\sum_{m_2} \frac{|\Omega_{1,m_1}^{2,m_2}(\boldsymbol{r})|^2}{\Delta_{1,m_1}^{2,m_2}(\boldsymbol{r})} , \quad V_{mw}^{2,m_2}(\boldsymbol{r}) = -\frac{\hbar}{4}\sum_{m_1} \frac{|\Omega_{1,m_1}^{2,m_2}(\boldsymbol{r})|^2}{\Delta_{1,m_1}^{2,m_2}(\boldsymbol{r})} . \tag{9.7}$$

As desired, the potentials for $F = 1$ and $F = 2$ have opposite signs, leading to a differential potential for the qubit states $|0\rangle \equiv |1, -1\rangle$ and $|1\rangle \equiv |2, 1\rangle$.

In addition to the magnetic microwave field, the electric field $\boldsymbol{E}_{\mathrm{mw}}(\boldsymbol{r})\cos(\omega t + \varphi)$ also leads to energy shifts. By averaging over the fast oscillation of the microwave at frequency ω, which is much faster than the atomic motion, the electric field leads to a time-averaged quadratic Stark shift. Hence, the total microwave potential for state $|0\rangle$, $u_0(\boldsymbol{r})$ in (9.4), is

$$u_0(\boldsymbol{r}) = -\frac{\alpha}{4}|\boldsymbol{E}_{\mathrm{mw}}(\boldsymbol{r})|^2 + \frac{\hbar}{4}\sum_{m_2=-2}^{0}\frac{\left|\Omega_{1,-1}^{2,m_2}(\boldsymbol{r})\right|^2}{\Delta_{1,-1}^{2,m_2}(\boldsymbol{r})}\,, \tag{9.8}$$

while the microwave potential for state $|1\rangle$ is

$$u_1(\boldsymbol{r}) = -\frac{\alpha}{4}|\boldsymbol{E}_{\mathrm{mw}}(\boldsymbol{r})|^2 - \frac{\hbar}{4}\sum_{m_1=0}^{+1}\frac{\left|\Omega_{1,m_1}^{2,+1}(\boldsymbol{r})\right|^2}{\Delta_{1,m_1}^{2,+1}(\boldsymbol{r})}\,. \tag{9.9}$$

The atom chip layout shown in Figure 9.4a allows one to realize the desired state-selective potential. It consists of two layers of gold metallization on a high resistivity silicon substrate, separated by a thin dielectric insulation layer. The wires carry stationary (DC) currents, which, when combined with appropriate stationary and homogeneous magnetic bias fields, create the state-independent potential $u_{\mathrm{c}}(\boldsymbol{r})$. In addition to carrying DC currents, the three wires on the upper gold layer form a coplanar waveguide (CPW) for a microwave at frequency ω. The microwave fields guided by these conductors create the state-dependent potential $u_k(\boldsymbol{r})$. The combination of DC and microwave currents in the same wires is possible by the use of bias injection circuits.

Making use of quantum optimal control techniques [48], a gate operation time $T_{\mathrm{g}} = 1.11\,\mathrm{ms}$ with a fidelity $F = 0.996$ can be obtained, as shown in [47]. We emphasize that with this T_{g} and the long coherence lifetime of the qubit pair chosen ($\sim 1\,\mathrm{s}$ at a few μm distance from the chip [7], see Section 9.3), thousands of gate operations can be accomplished. The fidelity calculation includes the effect of several error sources: trap losses and decoherence due to the chip surface, undesired two-photon transitions induced by the microwave, mixing of the hyperfine levels due to the microwave coupling, and qubit dephasing due to technical noise. In the limit of large microwave detuning, the admixture of other states with different magnetic moments to the qubit states is strongly reduced. A last important point is related to the difficulty to prepare the atoms in the vibrational ground state with close to 100 % efficiency. This effect, modeled by a finite temperature, has been also included in the analysis. For temperatures $T \leq 20\,\mathrm{nK}$ in the initial double-well trap, the fidelity is not reduced significantly.

A key ingredient of the quantum gate discussed here is the state-dependent microwave near-field potential. In a recent experiment [27], such a potential was realized on an atom chip, and it was used for the coherent manipulation of a two-component BEC in a superposition of the qubit states $|0\rangle$ and $|1\rangle$. The BEC was

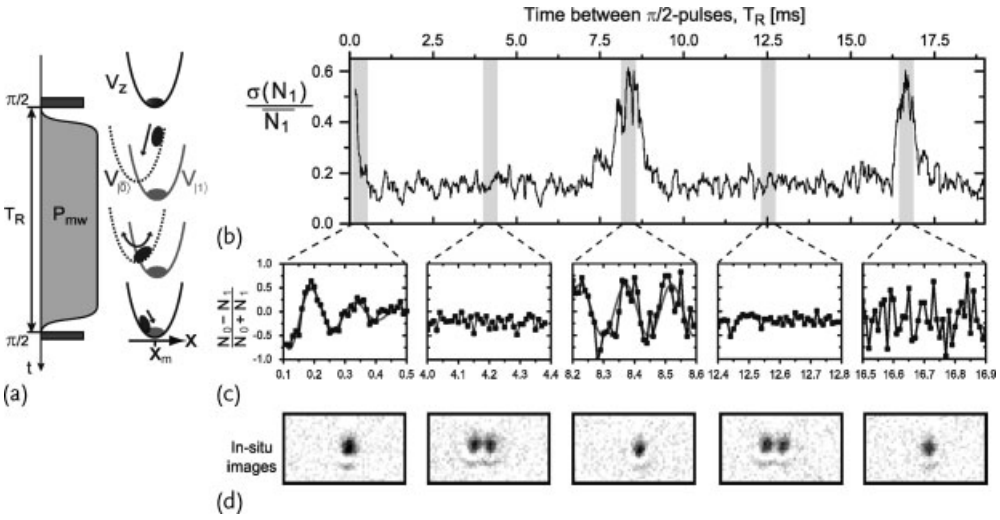

Figure 9.5 *Coherent state-dependent splitting and recombination of a BEC with microwave near-fields.* The contrast of Ramsey fringes on the $|0\rangle \leftrightarrow |1\rangle$ transition is modulated due to the periodic splitting and recombination of the motional wave function of the BEC. (a) Experimental sequence. (b) As a measure of the wave function overlap, $\sigma(N_1)/\bar{N}_1$ is shown as a function of T_R, where $\sigma(N_1)$ is the standard deviation and $\bar{N}_1$ the mean of N_1 obtained from a running average over one period of the Ramsey fringes. (c) Corresponding Ramsey fringe data for selected values of T_R. (d) In situ images of the atomic density distribution of $|0\rangle$ and $|1\rangle$, for T_R corresponding to the center of the windows in (c).

state-selectively split and recombined, entangling atomic internal and motional states in a reversible way, as required for the atom chip quantum gate. Figure 9.5a illustrates the experimental sequence. It consists of a Ramsey $\pi/2 - \pi/2$ sequence on the $|0\rangle \leftrightarrow |1\rangle$ transition in combination with state-dependent splitting and recombination of the motional wave functions. After the first $\pi/2$-pulse, the microwave on the CPW is switched on within 50 µs, which corresponds to a sudden displacement of the potential minimum for state $|0\rangle$ by 4.3 µm. The wave function of state $|0\rangle$ is thus set into oscillation in the shifted potential. After a variable delay, the microwave is switched off within 50 µs, followed by the second $\pi/2$-pulse and state-selective detection to determine the number of atoms N_0 (N_1) in state $|0\rangle$ ($|1\rangle$). Figures 9.5b–d show the experimental results. The Ramsey interference contrast is modulated by the wave function overlap of the two states and thus periodically vanishes and reappears again due to the oscillation of state $|0\rangle$. Precisely at the time when state $|0\rangle$ has performed a full oscillation a sharp recurrence of the contrast is observed. This recurrence of high-contrast interference fringes proves that the combined evolution of internal and motional state is coherent.

We conclude this section with a last remark. The scheme proposed in [49] for atoms confined in optical lattices could also be implemented with state-dependent microwave potentials. Here at time $t = 0$ the atom α in the logical state $|k\rangle$ experiences the potential $V_\alpha^k(\boldsymbol{r}, t) = V(\bar{\boldsymbol{r}}^k + \delta \boldsymbol{r}_\alpha^k(t) - \boldsymbol{r})$, which is initially ($t < 0$) centered at position $\bar{\boldsymbol{r}}_k$. The centers of the potentials move according to the trajec-

tories $\delta \boldsymbol{r}_\alpha^k(t)$ with the condition $\delta \boldsymbol{r}_\alpha^k(0) = \delta \boldsymbol{r}_\alpha^k(T_\mathrm{g}) = 0$, and such that the first atom collides with the second one if and only if they are in the logic states $|0\rangle$ and $|1\rangle$. Such a scheme could be implemented with microwave potentials by using a microwave state dressing scheme where only state $|0\rangle$ effectively couples to the microwaves, as for example in the experiment of [27].

9.7.2 Motional-State Qubits and Collisional Interactions

Based again on the conditional phase shifts induced by the collision between cold atoms, a number of proposals rely on the manipulation of quantum information stored in motional degrees of freedom. The original proposals [11, 12, 50] dealt with optical lattices, but those schemes can also be implemented using microscopic potentials on atom chips. Besides magnetic, microwave, or radio-frequency traps, chip-based optical traps are of interest in this context. By illuminating a 2D array of refractive or diffractive microlenses with laser light, a 2D set of diffraction-limited laser foci can be formed. Atoms can be confined in the optical dipole potentials generated by the laser foci [51]. In a first experiment, arrays with more than 80 sites were loaded with ensembles of about 1000 trapped ^{85}Rb atoms in the center of the 2D configuration and about 100 at the edges [52]. Theoretical proposals for two-qubit gates in this system rely again on the spatial overlap of two qubits out of initially separated locations. This can be accomplished by illuminating the array of microlenses with two laser beams with a finite relative angle of propagation creating two interleaved sets of dipole traps [51]. The variation of the relative angle yields a variation in the mutual distance between the trap sets. An important feature of these optical micropotentials is the relatively large separation of neighboring sites ($\sim 125\ \mu$m) which enables individual addressing [52].

In the quantum gate scheme of [50], a double-well potential contains one atom per well. The logic states $|0\rangle$ and $|1\rangle$ are identified with the single particle ground and excited states of each well, respectively. Initially the barrier is sufficiently high that tunneling between the lowest four eigenstates of a single trapped atom is negligible. When the barrier is lowered in such a way that the single particle excited states (the qubit state $|1\rangle$) of the potential do overlap, tunneling takes place and the energy shift due to the atom–atom interaction increases exponentially. The interaction lasts for a time sufficient to accumulate the required phase shift for a phase gate and subsequently the initial trapping configuration is restored by increasing the barrier again. An accurate use of quantum interference between two-particle states yields an optimized gate duration of 38 ms with an infidelity $1 - F \approx 6.3 \times 10^{-6}$. In the proposal of [11] the scenario is very similar and it uses the same qubit set. While in [50] the two-qubit gate is physically realized by lowering and increasing the barrier of the double-well potential, in [11] the (initially) separated traps adiabatically approach (or separate from) each other. In that way it is possible to obtain $T_\mathrm{g} \sim 20$ ms for a $\sqrt{\mathrm{SWAP}}$ two-qubit gate.

The proposal of [11, 12] uses again motional states, but not strictly the vibrational states of the trap. In the scheme each qubit consists of two separated traps

and a single atom. Now, the computational basis $\{|0\rangle, |1\rangle\}$ is formed in this way: the ground state of the left trap represents $|0\rangle \equiv |0\rangle_{\mathrm{L}}$, whereas the ground state of the right trap represents $|1\rangle \equiv |0\rangle_{\mathrm{R}}$. One- and two-qubit quantum gates are performed by adiabatically approaching the trapping potentials and allowing for tunneling to take place. We note that in such a scheme four wells are needed to implement a two-qubit gate, either arranged in a 1D configuration with the traps on a line or side-by-side in a 2D configuration. Taking into account the different error sources present in this scheme, like fluctuations of the trap positions, photon scattering, and heating, one obtains an error rate of about 0.02, with a single-qubit operation time of 4 ms, and $T_{\mathrm{g}} \sim 10$ ms for a two-qubit operation such as a phase gate. Even though the error rate is rather large, the scheme offers several advantages: (1) decoherence due to spontaneous emission reduces the fidelity only marginally; (2) no momentum transfer is effected for single and two-qubit gates; (3) a state-dependent interaction is not required for the implementation of two-qubit gates; (4) the readout is done with a laser beam focused onto one trap minimum and detecting the fluorescence light; (5) since one- and two-qubit gates are realized using the same technique, that is, by approaching the traps adiabatically, the complexity of the experimental setup would be reduced.

Both of these schemes can be implemented on an atom chip by means of a combination of static and microwave fields, with the need of trapping only one hyperfine level. However, one can combine the nice coherence properties of the qubit states $|F = 2, m_{\mathrm{F}} = 1\rangle$ and $|F = 1, m_{\mathrm{F}} = -1\rangle$ of the ground state of ^{87}Rb, and the entanglement produced by cold collisions via the motional states $(|g\rangle, |e\rangle)$. In [13] two different ways of realizing this concept have been proposed: (a) duplicate the logical state of the storage levels in the motional levels, where $|1g\rangle \leftrightarrow |1e\rangle$; (b) swap the logical states of the two degrees of freedom, $|1g\rangle \leftrightarrow |0e\rangle$. Here we consider only the swap scheme.

Given the initial state $|\varphi_0\rangle = (a|00\rangle + b|01\rangle + c|10\rangle + d|11\rangle)\,|gg\rangle$, the swap scheme takes place in three steps: (i) we selectively excite the operation state and de-excite the storage states $|\varphi_1'\rangle = |00\rangle\,(a|gg\rangle + b|ge\rangle + c|eg\rangle + d|ee\rangle)$, that is, we swap their logic states; then (ii) the operation states get a dynamical phase ϕ: $|\varphi_2'\rangle = |00\rangle\left(a|gg\rangle + b|ge\rangle + c|eg\rangle + \mathrm{e}^{\mathrm{i}\varphi} d|ee\rangle\right)$ through collisions; finally (iii) we swap again the storage and operation states $|\varphi_3'\rangle = \left(a|00\rangle + b|01\rangle + c|10\rangle + \mathrm{e}^{\mathrm{i}\varphi} d|11\rangle\right)$ $|gg\rangle$. Such a swap gate scheme is not restricted to internal and external degrees of freedom of cold atoms, but it can be applied to any system with at least two degrees of freedom. A selective excitation of vibrational states is required when cold atoms are employed. In order to realize it, the use of two-photon Raman transitions has been suggested. The experimental implementation of such transitions with ^{87}Rb atoms is rather delicate and a careful analysis is given in [14]. In a static version of the swap scheme, where the barrier is fixed and it is designed in such a way that the left and right single particle excited states overlap, an operation time for a phase gate of 16.25 ms with a gate fidelity $F > 0.99$ has been predicted [13]. In an optimized version of the gate dynamics, where the barrier is lowered and increased in order to get faster operation times for a desired value of infidelity, it has been possible to achieve fidelities of 0.99 in 6.3 ms and of 0.999 in 10.3 ms [14].

We conclude by noting that the concept of spatially delocalized qubits of [11] could also be used to implement discrete-time quantum walks [53].

9.7.3 Alternative Chip-Specific Approaches to Entanglement Generation

High-fidelity entanglement of cold neutral atoms can be achieved by combining several already available techniques such as the creation or dissociation of neutral diatomic molecules with the manipulation of atoms by linear atom optics elements that can be integrated on atom chips, like atomic beam splitters, phase shifters, and interferometers.

Let us consider the free-space decay of a two-atom system (e.g., a diatomic molecule) with zero total momentum. The two atoms will freely propagate along correlated directions due to momentum conservation: If one of the two atoms leaves along a specific direction, say from the left side a_1 with momentum $\boldsymbol{k}_a$, the remaining atom will certainly leave along the corresponding direction a_2 (opposite to a_1) with momentum $-\boldsymbol{k}_a$. However, the decay in free space leads to freely propagating atoms along many pairs of correlated directions such that the probability for the two atoms moving along any specified pair is small. By means of integrated, miniaturized atom optical devices on atom chips this drawback can be overcome. By restricting the decay to a limited phase space given by the atom optical microstructure one can reduce the available decay modes significantly to only the few desired modes. If there are only two directions the two atoms will move along, one can deterministically obtain the path-entangled state $|\Phi\rangle \propto |a_1, a_2\rangle + |b_1, b_2\rangle$, where $|a\rangle$ and $|b\rangle$ are two orthonormal spatial states of atoms [54].

For instance, a diatomic molecule can be guided into a molecule beam splitter, which can split the molecule into either path a or path b. In each of the one-dimensional guides, the molecule can be dissociated into correlated atoms, which will propagate along the two pairs of correlated directions. If the released decay energy for each atom is smaller than the transverse level spacing in the guides, the decay can only occur in the lowest energy state of the transverse modes, and it is restricted to only one mode per path. In this case each two-atom correlated decay leads to an atom pair entangled in the specified paths (spatial modes).

9.7.4 Cavity-QED-Based Schemes

Recent experimental advances in cavity QED on a chip have yielded results that promise the full integration and scalability of such cavities. Microscopic Fabry–Pérot cavities whose open structure gives access to the central part of the cavity field have been developed. In such cavities strong coupling between a single atom and the cavity mode has been obtained [37]. In these experiments a BEC was employed, which can be located deterministically everywhere in the cavity and positioned entirely within a single antinode of the standing-wave cavity mode field. This gives rise to a controlled and tunable coupling rate.

On the theoretical side, proposals for a quantum computer based on a cavity QED model have been put forward. The scheme of [55] assumes N atoms coupled to a single quantized mode of a high-finesse cavity. Quantum operations (e.g., a controlled-NOT gate) are realized via the coupling of the atoms with individual lasers and their entanglement is mediated by the exchange of a single cavity photon. In a similar setup a controlled-NOT gate can be performed through a sequence of (destructive) measurements on the atoms and quantum non-demolition measurements of the atom number [56]. Because of the randomness of the measurement outcome in this case the gate operation is probabilistic. Nevertheless, this scheme is more robust against decoherence and cavity losses than the one of [55]: while in that proposal the infidelity scales as $1/\sqrt{2C_0}$, in [56] it scales as $\log(2C_0)/2C_0$, where C_0 is the cooperativity parameter.

Another interesting possibility of quantum information processing is given by distributed quantum networks [57], whose nodes are optical cavities. This would allow for applications in entangled state cryptography, teleportation, purification and distributed quantum computation. The combination of integrated micro-optical cavities and optical fibers as transmission lines would allow the implementation of such networks also on atom chips.

9.7.5
Quantum Gate Schemes that Can Be Adapted from Other Contexts

Quantum gate proposals initially meant for systems confined in, for example, optical lattices such as the scheme for moving potentials discussed briefly in Section 9.7.1 can be also realized in on-chip optical lattices [58] or magnetic microtrap lattices [8, 9]. In Section 9.7.1 we suggested to move the centers of the traps by means of microwave potentials. The results of [58] show that it is possible to realize 1D and 2D optical lattices on a chip, where the traps are the nodes of the evanescent wave field above an optical waveguide resulting from the interference of different waveguide modes. With a laser power of $\sim$ 1 mW it is possible to produce tight traps, 150 nm above the on-chip waveguide surface, with trap frequencies on the order of 1 MHz, and with a spatial periodicity of about 1 μm. Moreover, the individual qubits are readily addressable, and it is possible to move 1D arrays of qubits by adjusting the phases of the waveguide modes. The drawback of such technology is that to get strong confinement with waveguides made from existing materials and using low laser powers, one needs to work extremely close to the waveguide surface implying a relevant impact on the qubit coherence. Alternatively one can use current-carrying wires and a perpendicularly magnetized grooved structure [8]. This solution allows for the trapping and cooling of ultra-cold atoms by means of the current-carrying wires, whereas the magnetic microstructure generates a 1D permanent magnetic lattice with a spacing between neighboring sites on the order of 10 μm and with trap frequencies of up to 90 kHz.

On the basis of such experimental achievements, schemes that exploit the interaction of atoms excited to low-lying Rydberg states [15] can be also used on atom chips [16]. An appropriate sequence of laser pulses above a waveguide can excite

the qubits into Rydberg states and entangle them via electric dipole–dipole interactions [58]. While the phase gate model suggested in [15] relies only on the strong dipole–dipole interaction, in another recent proposal [59] one can combine the Rydberg blockade mechanism with the rapid laser pulse sequence of the well-known stimulated Raman adiabatic passage (STIRAP). This combination with the engineering of a time-dependent relative phase $\phi_R(t)$ between the Rabi frequencies of the two STIRAP laser pulses affords a higher degree of control of the phase of Eq. (9.2) through the manipulation of geometrical phases.

So far, we discussed only qubits that are represented by individual two-level systems. This kind of qubits requires high control and addressability of individual particles, which raise important challenges for experimentalists. Some theoretical investigations, however, use a symmetric collective state of a mesoscopic atomic ensemble [17], where only one excitation is present in the system. The dipole excitation blockade mechanism of Rydberg atoms works in that direction, because it prevents multiple excitations in an ensemble. The same mechanism used to implement a fast phase gate with two Rydberg atoms can be extended to qubits stored in few-μm-spaced atomic clouds, where each atomic ensemble is a qubit. Alternatively, collective states in ensembles of multi-level quantum systems can be used to store the information [18]. Quantum operations such as one- and two-bit gates are then implemented by collective internal state transitions taking place in the presence of an excitation blockade mechanism, such as the one provided by the Rydberg blockade.

Another interesting solution to the issue of single-atom addressability via a laser is quantum computation with neutral atoms, based on the concept of 'marker' atoms, that is, auxiliary atoms that can be efficiently transported in state-independent periodic external traps to operate quantum gates between physically distant qubits [48]. Here, again, qubits are represented by internal long-lived atomic states, and qubit atoms are stored in a regular array of microtraps. These qubit atoms remain frozen at their positions during the quantum computation. In addition to the atoms representing the qubits, an auxiliary 'marker atom' (or a set of marker atoms) is considered, which can be moved between the different lattice sites containing the qubits. The marker atoms can either be of a different atomic species or of the same type as the qubit atoms, but possibly employing different internal states. These movable atoms serve two purposes. First, they allow addressing of atomic qubits by 'marking' a single lattice site due to the marker qubit interactions: the corresponding molecular complex can be manipulated with a laser without the requirement of focusing on a particular site. Second, the movable atoms play the role of 'messenger' qubits which allow one to transport quantum information between different sites in the optical lattice, and thus to entangle distant atomic qubits. The required qubit manipulation and trapping techniques for such a scheme are essentially the same as the ones previously presented, and it is therefore well suited for atom chips.

9.8
Hybrid Approaches to QIP on a Chip

Atom chips are ideally suited as a platform for hybrid approaches to QIP, in which different systems such as neutral atoms, ions, photons, and solid-state systems are combined. In fact, one could argue that chip traps for atoms, ions and molecules are the enabling technology which makes such hybrid approaches possible.

9.8.1
Hybrid Approaches to Entanglement Generation

Atomic or molecular qubits trapped on an atom chip could be coupled to solid-state systems for QIP on the chip surface. The resulting hybrid quantum systems would combine fast processing (solid state) with long coherence times (atomic or molecular systems). Many interesting combinations of systems are conceivable. The proposals of [20–24, 60] suggest to use superconducting wires or superconducting microwave cavities to 'wire up' several atomic qubits or to couple atomic qubits to a Cooper pair box on the chip surface. The atomic systems considered in this context are Rydberg atoms [23], atomic ions [60], polar molecules [20, 22, 24], and ground-state neutral atoms [21].

In this context, the proposal of [24] suggests an extension of the atom chip concept to ultra-cold polar molecules. It proposes a scalable cavity-QED-type quantum computer architecture, where entanglement of distant qubits stored in long-lived rotational molecular states is achieved via exchange of microwave photons. Polar molecules have stable internal states that can be controlled by electrostatic fields. This controllability is due to their rotational degree of freedom in combination with the asymmetry of their structure (unlike atoms). By applying moderate laboratory electric fields, rotational states with transition frequencies in the microwave range can be mixed, and the molecules acquire large dipole moments, which are the key property that makes them effective qubits in a quantum processing system. Furthermore, the application of electric field gradients leads to large mechanical forces, allowing one to trap the molecules. For instance, the electrostatic Z-trap for polar molecules proposed in [24] creates a non-zero electric field minimum in close proximity to the surface, analogous to Ioffe–Pritchard-type magnetic traps for neutral atoms.

In [21], a related idea is put forward involving an ensemble of ultra-cold neutral atoms coupled magnetically to a superconducting microwave resonator. Strong coupling between a single microwave photon in the coplanar waveguide resonator and a collective hyperfine qubit state in the atomic ensemble could be achieved. Integrated on an atom chip, such a system could be used to interconnect solid-state and atomic qubits and to perform a range of interesting cavity quantum electrodynamics experiments.

The proposals of [20, 22] suggest a quantum computer model where ensembles of cold molecules are used as a stable quantum memory by means of collective spin states, whereas a Cooper pair box, connected to the molecular ensemble via a strip-

line cavity, is used to perform one- and two-qubit operations and readout. In [20] the ground state and a symmetric collective state with only one excitation present in the ensemble are the qubit states, and therefore an ensemble of molecules carries only two logic states. On the other hand, in [22] a 'holographic quantum register' is encoded in collective excitations with defined spatial phase variations, where each phase pattern is addressed by optical Raman processes with classical fields. This allows one to store hundreds of qubits in just one sample. This way of encoding does not pose special problems for an atom chip implementation, where usually single-atom addressing with laser beams is required.

9.8.2
Interfacing Atoms (Storage/Processing Qubits) with Photons (Flying Qubits)

Strong atom–photon coupling has been demonstrated with trapped atoms in an on-chip cavity [37]. Such a system could be used to interface storage/processing qubits and flying qubits. In a similar way, microwave cavities could be employed as a quantum bus on the chip, as described in the previous section, where a collective atomic quantum state can be mapped into a photonic state and vice versa. With such on-chip cavities quantum networks as described in Section 9.7.4 can be realized. Quite interesting is also the possibility offered by integrated cavities to perform quantum non-demolition measurements of the BEC atom number, therefore allowing the preparation of atomic quantum superposition states [61]. Additionally, by employing Raman transitions for transferring a small and exact known number N of BEC atoms into a different internal state, it is possible, by means of a transverse (to the cavity axis) laser beam, to convert such N condensed atoms into a N-photon Fock state, which would allow the deterministic production of photons [37].

9.8.3
Quantum Information Technology for Precision Measurement and Other Applications

Quantum information technology, in particular techniques for coherent manipulation and entanglement generation, already find applications in other areas of science. In the currently emerging field of quantum metrology [62], many-particle entanglement in the form of spin-squeezed states is investigated as a way to overcome the standard quantum limit of interferometric measurement, which limits today's best atomic clocks. Techniques originally developed for QIP on atom chips enable such experiments with chip-based atomic clocks and interferometers.

A class of hybrid systems which is interesting in the context of precision measurement are atoms coupled to micro- or nano-mechanical oscillators [63–65]. Mechanical oscillators have applications in ultra-sensitive force detection. A strongly coupled atom-oscillator system provides a quantum interface allowing the coherent transfer of quantum states between the mechanical oscillator and atoms, opening the door to coherent manipulation, preparation, and measurement of micromechanical objects via the well-developed tools of atomic physics.

9.9 Conclusion and Outlook

When the first atom chip experiments were performed, quantum information processing was already considered a promising direction for future applications. A significant number of theoretical proposals for implementing quantum gates on an atom chip have since then been put forward, and we have tried to review them in this chapter. Several of these proposals have been worked out in detail, including investigations of various kinds of imperfections such as decoherence due to atom–surface interactions. High-fidelity quantum gates compatible with the requirements for fault-tolerant QIP seem experimentally feasible on atom chips even in the presence of these imperfections. Moreover, ideas and techniques developed for QIP are now also being investigated with great success in the context of quantum metrology or quantum simulations with atom chips.

On the experimental side, impressive progress was made in the chip-based coherent control of ultra-cold atoms. Coherent manipulation of long-lived hyperfine qubit states was demonstrated close to a chip surface [7], and coherent control of motional states is routinely achieved in chip-based atom interferometers (see Chapter 7). Chip-based lattices were created [9] which could store a large register of qubits. The experimental achievement of strong coupling of atoms to a chip-based optical cavity [35, 37] paves the way for deterministic single-atom control. In a recent experiment, ultra-cold atoms were coherently manipulated with an internal-state-dependent potential on an atom chip [27], a key ingredient of the proposed quantum gate of [42, 47]. An important experimental milestone for the near future is the controlled generation of entanglement between atoms on a chip.

While the development of chip-based near-field traps was pioneered for ultra-cold neutral atoms, it has already triggered similar developments for other systems such as ions or molecules. As trapped ions are currently one of the frontrunners in the field of QIP, the recent demonstration of chip-based ion traps is particularly exciting (see Chapter 13). One of the most promising directions of future research is the development of hybrid architectures for QIP, where the advantageous features of neutral atoms, ions, photons, and solid-state systems are combined in a single chip-based device. The many beautiful experiments on atom chips reported in this book have been an essential inspiration for this development.

References

1 Nielsen, M.A. and Chuang, I.L. (2000) *Quantum Computation and Quantum Information*, Cambridge University Press, Cambridge.

2 Schmiedmayer, J., Folman, R., and Calarco, T. (2002) Quantum information processing with neutral atoms on an atom chip. *J. Mod. Opt.* **49**, 1375.

3 DiVincenzo, D. (2000) The Physical Implementation of Quantum Computation. *Fortschr. Phys.* **48**, 771.

4 Treutlein, P., Steinmetz, T., Colombe, Y., Lev, B., Hommelhoff, P., Reichel, J., Greiner, M., Mandel, O., Widera, A., Rom, T., Bloch, I., and Hänsch, T.W. (2006) Quantum information process-

ing in optical lattices and magnetic microtraps. *Fortschr. Phys.* **54**, 702.
5 Steane, A. (2003) Overhead and noise threshold of fault-tolerant quantum error correction. *Phys. Rev. A* **68**, 42322.
6 Knill, E. (2005) Scalable quantum computing in the presence of large detected-error rates. *Phys. Rev. A* **71**, 42322.
7 Treutlein, P., Hommelhoff, P., Steinmetz, T., Hänsch, T.W., and Reichel, J. (2004) Coherence in microchip traps. *Phys. Rev. Lett.* **92**, 203005.
8 Singh, M., Volk, M., Akulshin, A., Sidorov, A., McLean, R., and Hannaford, P. (2008) One-dimensional lattice of permanent magnetic microtraps for ultracold atoms on an atom chip. *J. Phys. B: At. Mol. Opt. Phys.* **41**, 065301.
9 Whitlock, S., Gerritsma, R., Fernholz, T., and Spreeuw, R.J.C. (2009) Two-dimensional array of microtraps with atomic shift register on a chip. *New. J. Phys.* **11**, 023021.
10 Lengwenus, A., Kruse, J., Volk, M., Ertmer, W., and Birkl, G. (2007) Coherent manipulation of atomic qubits in optical micropotentials. *Appl. Phys. B* **86**, 377.
11 Eckert, K., Mompart, J., Yi, X.X., Schliemann, J., Bruß, D., Birkl, G., and Lewenstein, M. (2002) Quantum computing in optical microtraps based on the motional states of neutral atoms. *Phys. Rev. A* **66**, 042317.
12 Mompart, J., Eckert, K., Ertmer, W., Birkl, G., and Lewenstein, M. (2003) Quantum computing with spatially delocalized qubits. *Phys. Rev. Lett.* **90**, 147901.
13 Cirone, M.A., Negretti, A., Calarco, T., Krüger, P., and Schmiedmayer, J. (2005) A simple quantum gate with atom chips. *Eur. Phys. J. D* **35**, 165.
14 Charron, E., Cirone, M.A., Negretti, A., Schmiedmayer, J., and Calarco, T. (2006) Theoretical analysis of a realistic atom-chip quantum gate. *Phys. Rev. A* **74**, 012308.
15 Jaksch, D., Cirac, J.I., Zoller, P., Rolston, S.L., Côté, R., and Lukin, M.D. (2000) Fast quantum gates for neutral atoms. *Phys. Rev. Lett.* **85**, 2208.
16 Mozley, J., Hyafil, P., Nogues, G., Brune, M., Raimond, J.-M., and Haroche, S. (2005) Trapping and coherent manipulation of a Rydberg atom on a microfabricated device: a proposal. *Eur. Phys. J. D* **35**, 43.
17 Lukin, M.D., Fleischhauer, M., Cote, R., Duan, L.M., Jaksch, D., Cirac, J.I., and Zoller, P. (2001) Dipole blockade and quantum information processing in mesoscopic atomic ensembles. *Phys. Rev. Lett.* **87**, 037901.
18 Brion, E., Mølmer, K., and Saffman, M. (2007) Quantum computing with collective ensembles of multilevel systems. *Phys. Rev. Lett.* **99**, 260501.
19 Yan, H., Yang, G., Shi, T., Wang, J., and Zhan, M. (2008) Quantum gates with atomic ensembles on an atom chip. *Phys. Rev. A* **78**, 034304.
20 Rabl, P., DeMille, D., M. Doyle, J., Lukin, M.D., Schoelkopf, R.J., and Zoller, P. (2006) Hybrid quantum processors: Molecular ensembles as quantum memory for solid state circuits. *Phys. Rev. Lett.* **97**, 033003.
21 Verdú, J., Zoubi, H., Koller, C., Majer, J., and Ritsch, H. (2009) Strong magnetic coupling of an ultracold gas to a superconducting waveguide cavity. *Phys. Rev. Lett.* **103**, 043603.
22 Tordrup, K., Negretti, A., and Mølmer, K. (2008) Holographic quantum computing. *Phys. Rev. Lett.* **101**, 40501.
23 Sørensen, A.S., van der Wal, H.C., Childress, L.I., and Lukin, M.D. (2004) Capacitive coupling of atomic systems to mesoscopic conductors. *Phys. Rev. Lett.* **92**, 063601.
24 Andre, A., DeMille, D., Doyle, J.M., Lukin, M.D., Maxwell, S.E., Rabl, P., Schoelkopf, R.J., and Zoller, P. (2006) A coherent all-electrical interface between polar molecules and mesoscopic superconducting resonators. *Nat. Phys.* **2**, 636.
25 Steffen, M., Ansmann, M., Bialczak, R.C., Katz, N., Lucero, E., McDermott, R., Neeley, M., Weig, E.M., Cleland, A.N., and Martinis, J.M. (2006) Measurement of the entanglement of two superconducting qubits via state tomography. *Science* **313**, 1423.
26 Majer, J., Chow, J.M., Gambetta, J.M., Koch, J., Johnson, B.R., Schreier, J.A.,

Frunzio, L., Schuster, D.I., Houck, A.A., Wallraff, A., Blais, A., Devoret, M.H., Girvin, S.M., and Schoelkopf, R.J. (2007) Coupling superconducting qubits via a cavity bus. *Nature* **449**, 443.

27 Böhi, P., Riedel, M.F., Hoffrogge, J., Reichel, J., Hänsch, T.W., and Treutlein, P. (2009) Coherent manipulation of Bose-Einstein condensates with state-dependent microwave potentials on an atom chip. *Nat. Phys.* **5**, 592.

28 Wineland, D.J., Monroe, C., Itano, W.M., Leibfried, D., King, B.E., and Meekhof, D.M. (1998) Experimental issues in coherent quantum-state manipulation of trapped atomic ions. *J. Res. Natl. Inst. Stand. Technol.* **103**, 259.

29 Morinaga, M., Bouchoule, I., Karam, J.C., and Salomon, C. (1999) Manipulation of motional quantum states of neutral atoms. *Phys. Rev. Lett.* **83**, 4037.

30 Wang, Y.-J., Anderson, D.Z., Bright, V.M., Cornell, E.A., Diot, Q., Kishimoto, T., Prentiss, M., Saravanan, R.A., Segal, S.R., and Wu, S. (2005) Atom Michelson interferometer on a chip using a Bose–Einstein condensate. *Phys. Rev. Lett.* **94**, 090405.

31 Hofferberth, S., Lesanovsky, I., Fischer, B., Verdu, J., and Schmiedmayer, J. (2006) Radiofrequency-dressed-state potentials for neutral atoms. *Nat. Phys.* **2**, 710.

32 Stibor, A., Kraft, S., Campey, T., Komma, D., Günther, A., Fortágh, J., Vale, C.J., Rubinsztein–Dunlop, H., and Zimmermann, C. (2007) Calibration of a single-atom detector for atomic microchips. *Phys. Rev. A* **76**, 033614.

33 Wilzbach, M., Heine, D., Groth, S., Liu, X., Hessmo, B., and Schmiedmayer, J. (2008) A simple integrated single-atom detector, preprint arXiv:0801.3255.

34 Teper, I., Lin, Y.-J., and Vuletić, V. (2006) Resonator-aided single-atom detection on a microfabricated chip. *Phys. Rev. Lett.* **97**, 023002.

35 Aoki, T., Dayan, B., Wilcut, E., Bowen, W.P., Parkins, A.S., Kippenberg, T.J., Vahala, K.J., and Kimble, H.J. (2006) Observation of strong coupling between one atom and a monolithic microresonator. *Nature* **443**, 671.

36 Steinmetz, T., Colombe, Y., Hunger, D., Hänsch, T.W., Balocchi, A., Warburton, R.J., and Reichel, J. (2006) Stable fiber-based Fabry–Pérot cavity. *Appl. Phys. Lett.* **89**, 111110.

37 Colombe, Y., Steinmetz, T., Dubois, G., Linke, F., Hunger, D., and Reichel, J. (2007) Strong atom-field coupling for Bose–Einstein condensates in an optical cavity on a chip. *Nature* **450**, 272.

38 Trupke, M., Goldwin, J., Darquie, B., Dutier, G., Eriksson, S., Ashmore, J., and Hinds, E.A. (2007) Atom detection and photon production in a scalable, open, optical microcavity. *Phys. Rev. Lett.* **99**, 063601.

39 Diener, R.B., Wu, B., G. Raizen, M., and Niu, Q. (2002) Quantum tweezer for atoms. *Phys. Rev. Lett.* **89**, 070401.

40 Mohring, B., Bienert, M., Haug, F., Morigi, G., Schleich, W.P., and Raizen, M.G. (2005) Extracting atoms on demand with lasers. *Phys. Rev. A* **71**, 053601.

41 Schlosser, N., Reymond, G., and Grangier, P. (2002) Collisional blockade in microscopic optical dipole traps. *Phys. Rev. Lett.* **89**, 023005.

42 Calarco, T., Hinds, E.A., Jaksch, D., Schmiedmayer, J., Cirac, J.I., and Zoller, P. (2000) Quantum gates with neutral atoms: Controlling collisional interactions in time-dependent traps. *Phys. Rev. A* **61**, 022304.

43 Calarco, T., Briegel, H.-J., Jaksch, D., Cirac, J., and Zoller, P. (2000) Quantum computing with trapped particles in microscopic potentials. *Fortschr. Phys.* **48**, 945.

44 Calarco, T., Briegel, H.-J., Jaksch, D., Cirac, J.I., and Zoller, P. (2000) Entangling neutral atoms for quantum information processing. *J. Mod. Opt.* **47**, 2137.

45 Calarco, T., Cirac, J.I., and Zoller, P. (2001) Entangling ions in arrays of microscopic traps. *Phys. Rev. A* **63**, 062304.

46 Negretti, A., Calarco, T., Cirone, M.A., and Recati, A. (2005) Performance of quantum phase gates with cold trapped atoms. *Eur. Phys. J. D* **32**, 119.

47 Treutlein, P., Hänsch, T.W., Reichel, J., Negretti, A., Cirone, M.A., and Calarco,

T. (2006) Microwave potentials and optimal control for robust quantum gates on an atom chip. *Phys. Rev. A* **74**, 022312.

48 Calarco, T., Dorner, U., Julienne, P.S., Williams, C.J., and Zoller, P. (2004) Quantum computations with atoms in optical lattices: Marker qubits and molecular interactions. *Phys. Rev. A* **70**, 012306.

49 Jaksch, D., Briegel, H.-J. Cirac, J.I., Gardiner, C.W., and Zoller, P. (1999) Entanglement of atoms via cold controlled collisions. *Phys. Rev. Lett.* **82**, 1975.

50 Charron, E., Tiesinga, E., Mies, F., and Williams, C. (2002) Optimizing a phase gate using quantum interference. *Phys. Rev. Lett.* **88**, 077901.

51 Birkl, G. and Fortágh, J. (2007) Micro traps for quantum information processing and precision force sensing. *Laser Photon. Rev.* **1**, 12.

52 Dumke, R., Volk, M., Müther, T., Buchkremer, F.B.J., Birkl, G., and Ertmer, W. (2002) Micro-optical realization of arrays of selectively addressable dipole traps: A scalable configuration for quantum computation with atomic qubits. *Phys. Rev. Lett.* **89**, 097903.

53 Eckert, K., Mompart, J., Birkl, G., and Lewenstein, M. (2005) One- and two-dimensional quantum walks in arrays of optical traps. *Phys. Rev. A* **72**, 012327.

54 Zhao, B., Chen, Z.-B., Pan, J.-W., Schmiedmayer, J., Recati, A., Astrakharchik, G.E., and Calarco, T. (2007) High-fidelity entanglement via molecular dissociation in integrated atom optics. *Phys. Rev. A* **75**, 042312.

55 Pellizzari, T., Gardiner, S.A., Cirac, J.I., and Zoller, P. (1995) Decoherence, continuous observation, and quantum computing: A cavity QED model. *Phys. Rev. Lett.* **75**, 3788.

56 Sørensen, A.S. and Mølmer, K. (2003) Measurement induced entanglement and quantum computation with atoms in optical cavities. *Phys. Rev. Lett.* **91**, 097905.

57 Cirac, J.I., Zoller, P., Kimble, H.J., and Mabuchi, H. (1997) Quantum state transfer and entanglement distribution among distant nodes in a quantum network. *Phys. Rev. Lett.* **78**, 3221.

58 Christandl, K., Lafyatis, G.P., Lee, S.-C., and Lee, J.-F. (2004) One- and two-dimensional optical lattices on a chip for quantum computing. *Phys. Rev. A* **70**, 032302.

59 Møller, D., Madsen, L.B., and Mølmer, K. (2008) Quantum gates and multiparticle entanglement by Rydberg excitation blockade and adiabatic passage. *Phys. Rev. Lett.* **100**, 170504.

60 Tian, L., Rabl, P., Blatt, R., and Zoller, P. (2004) Interfacing quantum-optical and solid-state qubits. *Phys. Rev. Lett.* **92**, 247902.

61 Nielsen, A.E.B., Poulsen, U.V., Negretti, A., and Mølmer, K. (2009) Atomic quantum superposition state generation via optical probing. *Phys. Rev. A* **79**, 023841.

62 Giovannetti, V., Lloyd, S., and Maccone, L. (2004) Quantum-enhanced measurements: Beating the standard quantum limit. *Science* **306**, 1330.

63 Tian, L. and Zoller, P. (2004) Coupled ion-nanomechanical systems. *Phys. Rev. Lett.* **93**, 266403.

64 Treutlein, P., Hunger, D., Camerer, S., Hänsch, T.W., and Reichel, J. (2007) Bose–Einstein condensate coupled to a nanomechanical resonator on an atom chip. *Phys. Rev. Lett.* **99**, 140403.

65 Hammerer, K., Wallquist, M., Genes, C., Ludwig, M., Marquardt, F., Treutlein, P., Zoller, P., Ye, J., and Kimble, H.J. (2009) Strong coupling of a mechanical oscillator and a single atom. *Phys. Rev. Lett.* **103**, 063005.